

IEEE 802.11
Wireless Access Method and Physical Layer Specification

Title: Update of Propagation Losses and Impulse Response of the Indoor Optical Channel

Authors: Cipriano R. A. T. Lomba, Rui T. Valadas, A.M. de Oliveira Duarte

Integrated Broadband Communications Group
Dept. of Electronics and Telecommunications
University of Aveiro
3800 AVEIRO
PORTUGAL

Tel: +351 34 381937
Fax: +351 34 381941
email: cipl@zeus.ci.ua.pt

Abstract

This paper is an update of a contribution previously presented [1] and further discusses the modelling, characterization and simulation of indoor wireless optical channels. The channel models used and the simulation package developed are presented. The propagation losses of indoor optical channels are considered. These are important for the evaluation of the system power budget. Minimization of the maximum channel propagation losses by optimizing the source emitting pattern is considered. The simulation package is also used to evaluate the impulse response and the bandwidth of the channel. We illustrate the use of the package by means of two case studies corresponding to: i) a satellite based cell and ii) a passive reflection based cell. It is seen that optimization of the emitting pattern by tuning the number, orientation and radiation pattern of the LEDs can significantly reduce the maximum channel losses and increase the channel bandwidth. Finally, the package is used to optimize the source emitting pattern of a system and to evaluate the collected power at each point of a particular room. The simulation results are compared with experimental results measured on that room.

This work is being carried out as part of the ESPRIT.6892 - POWER (Portable Workstation for Education in Europe) project commissioned by the CEC.

I - Introduction

Recently infrared technology based systems for indoor applications have been receiving significant interest. This resulted on the development of many new wireless systems using infrared technology for home, office and factory applications. The use of infrared technology presents some advantages over radio technology based systems. The main advantages are: easier to implement, do not require any licensing and are not affected by electromagnetic noise interference.

This paper presents mainly the evolution of a work presented previously [1]. It contains new simulation results of the propagation losses and channel impulse response for a few cases of indoor optical channels. In section II, the models of the optical channel and the main characteristics of the simulation package are briefly presented. In section III, we illustrate the use of the

simulation package by means of two case studies. The channel propagation losses, impulse response and frequency response are presented. The effects of the minimization of the maximum propagation losses and higher order reflections on the main characteristics of the channel are discussed. In section IV, we present a simulation case where the channel propagation losses of a particular channel are minimized and the collected power at each room position is simulated. Then, the simulation results are compared with experimental results. Finally, in section V we present the main conclusions of the simulation results.

This work is being carried out as part of the ESPRIT.6892 - POWER (Portable Workstation for Education in Europe) project commissioned by the CEC.

II - Models of the Indoor Optical Channel

In this section, the model of the optical indoor channel used in the simulation package is presented. The model includes the characteristics of the emitted optical beam, the effects of the channel over that beam and the receiver collecting characteristics. The channel propagation model is discussed in some detail and the expression used on the package for the evaluation of the channel impulse response is presented. The source and receiver models are the same as the discussed in reference [1] and are included here only for completeness.

1) The source model

Indoor infrared communication systems usually make use of short wavelength (820-900 nm) Light Emitting Diodes (LEDs). Following Gfeller [2], the radiant intensity of a LED can be modelled using an extension of the Lambertian law given by:

$$E(\phi) = \frac{(n+1)}{2 \times \pi} P_t \cos^n(\phi) \quad (1)$$

where P_t (usually supplied by the manufacturer data sheets) is the total emitted power, ϕ is the angle with the normal to the LED lens and n is a parameter indicating the beam width and is given by

$$n = -\frac{0.693}{\ln[\cos(HPBW)]} \quad (2)$$

where $HPBW$ is the LED half power emission angle. The first term on Eqn. (1) is a normalizing factor to assure that the total power radiated on the hemisphere equals P_t . For $HPBW=60^\circ$ n is unity and Eqn. (1) reduces to the case of the ideal Lambertian radiator. The higher the value of n the more directive is the radiation pattern of the LED. Figure 1 shows the radiation pattern of an ideal Lambertian LED, $\cos(\phi)$ curve, and of a more directive LED, $\cos^n(\phi)$ curve where $n>1$.

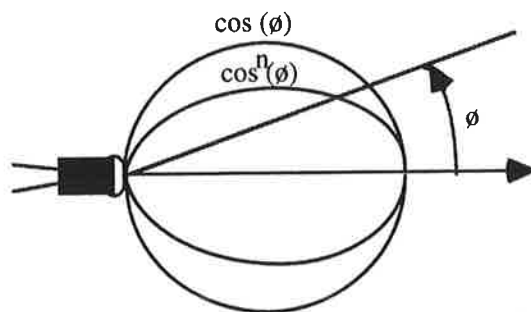


Figure 1 - The generalized Lambertian LED model

2) The Channel Propagation Model

There are mainly two independent factors influencing the channel propagation characteristics: the free-space propagation losses and the signal reflections on the room surfaces. The free-space losses under consideration are described by the $1/r^2$ law. Other characteristics of atmospheric systems, like signal attenuation, dispersion and scattering, are not considered since the ranges of indoor systems are very small and those effects are negligible.

The indoor infrared propagation channel is essentially a multipath channel: if the source emits a very short pulse, like a Dirac delta function, the collected signal at the receiver will be like a train of pulses, with different delays and amplitudes. This results from multiple reflections of the emitted pulse on the room walls, furniture, people and any other objects.

The model of the indoor propagation channel may be represented by a discrete low pass impulse response. The simulation package considers several reflection orders and the impulse response can be expressed as

$$h(t) = \sum_{i=0}^n \sum_{k=0}^m a_k \delta(t - \tau_k) \quad (3)$$

where n is the maximum number of signal reflections considered on the simulation, i is the signal reflection order, k is the path index, m is the total number of paths considered for the i th-reflection order, a_k represents the gain factor of the path also called *form-factor*, τ_k represents the path propagation delay and $\delta(t)$ is the Dirac delta function. The number total of paths, m , to consider depends mainly on the room dimensions, surface characteristics and on the emitting source characteristics.

The simulation model considers the signal power that goes into the receiver after being reflected up to n times. The line of sight collected power is considered when $i = 0$, m is also zero because there is only one path to consider (the emitter to receiver path). The evaluation of the collected power from each order of reflection considers always the power distribution due to the previous reflection. This distribution has to be considered as a space distribution and also as a time distribution due to different delays for different paths. Therefore, the a_k and the τ_k have to take into account the cumulative values resulting from the signal reflections of orders lower than the one that is being considered.

The value of the form-factors, a_k , on Eqn (3) depends on the source emitting characteristics, room dimensions and mainly on the surface reflection characteristics. The reflection characteristics of any surface depends upon the surface material and texture. To model accurately the reflection pattern of the most common surfaces the reflection model has to consider two components: a non-directional or diffuse term and a directional or specular term. This is achieved by considering the reflection coefficient as a sum of two terms [8]

$$R(\theta_{in}, \theta_{out}) = R_{d,out}(\theta_{in}) + R_{s,out}(\theta_{in}, \theta_{out}) \quad (4)$$

where the first term represents the signal reflected diffusely and the second term the signal reflected specularly. Solving for the diffuse and specular terms we have

$$R(\theta_{in}, \theta_{out}) = k_d \int_{\Omega} \rho_d I_{in}(\theta_{in}) \cos(\alpha) d\Omega + k_s \int_{\Omega} \rho_s(\theta_{in}, \theta_{out}) I_{in}(\theta_{in}) \cos(\alpha) d\Omega \quad (5)$$

where k_d is the fraction of radiation reflected diffusely and k_s is the fraction of the radiation reflected specularly, ($k_d + k_s = 1$). The factor ρ_d is the surface diffuse reflection coefficient and $\rho_s(\theta_{in}, \theta_{out})$ is the surface specular reflection coefficient. The sum of ρ_d and $\rho_s(\theta_{in}, \theta_{out})$ represents the *bi-directional reflectance function* of the reflecting surface. It represents also the

surface reflection coefficient as a function of the incoming direction, θ_{in} , and outgoing direction, θ_{out} . The factor $I_{in}(\theta_{in})$ represents the incident irradiance on the reflecting surface. θ is the angle between the incoming direction and the surface normal and $d\omega$ is the differential solid angle through which the incoming intensity arrives.

An accurate evaluation of this model imposes very strong requirements in terms of computing resources. Several simplified models describing the reflection properties of typical surfaces are available from the literature [6]. The most appropriate model to use depends on the surface characteristics and also on the complexity of the model we are able to implement.

We will consider that all the radiation is reflected diffusely, therefore, only the first term of Eqn. (5) is considered. This model is characteristic of perfectly diffusing surfaces and is called Lambertian reflection model. It has been shown that this model is a good approximation for most surfaces [2].

3) The Detector Model

In indoor wireless infrared systems, the most used detectors are large area silicon *Positive-Intrinsic-Negative*, *PIN*, photodetectors. To achieve larger collecting areas, without increasing the *PIN* capacitance, a lens to concentrate the incident radiation on the detector active area can also be employed. In both cases, the detector is modelled as having an active area which collects the power incident for angles smaller than the *FOV*, as represented in Figure 2. In the case of a lens being in use the transmittance factor of the lens has to be considered.

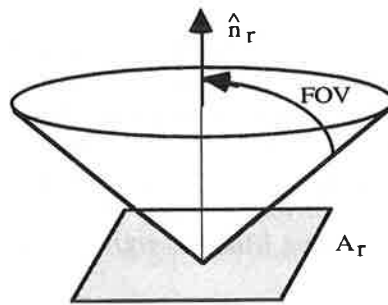


Figure 2 - Detector simulation model.

4) The Simulation Package

Based on the models of the indoor optical channel discussed above we have developed a simulation package. This package evaluates both the propagation losses and the impulse response of indoor optical channels.

The input parameters of the simulation package are:

- The source position, orientation and emitting pattern.
- The room dimensions and the reflection characteristics of the room surfaces.
- The receiver position, orientation and collecting characteristics.

The output parameters of the simulation package are:

- Power distribution over a plane.
- Maximum channel propagation losses.

- Power collected at any room position.
- Contribution of each reflection order for the total collected power.
- Channel impulse response.
- Channel transfer function.

The package evaluates the power distribution over the cell area. In addition, it allows for the optimization of the power distribution through the selection of the most appropriate parameters of the emitter and receiver arrays. The optimization process has in view the reduction of the worst-case propagation losses. This process considers the line-of-sight power distribution if the system uses active reflection and only the power distribution due to the ceiling reflection if passive reflection is used. These results are used to establish the system power budget.

The channel impulse response is a key factor in the design of infrared indoor systems operating at data rates higher than a few Mbit/s. The package allows the evaluation of the channel impulse response and transfer function. For that purpose, multiple-order reflections from the room walls are considered as we explained in section 2. The package allows the user to consider up to 5 reflections in the evaluation of the channel impulse response. The package allows also to determine the contribution of each reflection order for the total collected power and its influence on the main channel characteristics. This package is still being improved.

The simulation of the impulse response of indoor optical channels requires high resolution and a very large number of incremental areas have to be considered. This factor requires the use of simplified reflection models and results in a simulation package with very demanding computational resources. On the package, a compromise between CPU processing time and memory requirements had to be considered. Thus, data is processed on the fly, i.e. sorting of data is done automatically using an indexed array, and lookup tables are used. Due to computational requirements the evaluation of the impulse response only considers empty rooms.

III - Case Studies

The simulation package was used for simulation of a small room (5 by 5 by 3 meters) which had been previously simulated at the University of California, Berkeley [5] using their own simulation software. The results of both simulations were in very good agreement which indicates the simulation package is operating correctly.

The simulation package discussed above is now used in the evaluation and minimization of the channel propagation losses for two case studies corresponding to: a system with a satellite and a passive reflection based system. The optimization variable will be the emitter radiation pattern, i.e., the number, orientation and radiation pattern of the LEDs forming the optical source. The package is also used to evaluate the impulse response and transfer function of the indoor infrared channel.

A - System with Active Reflection

This case is representative of indoor infrared systems where the ceiling surface does not reflect the infrared radiation properly or an extension of the coverage area of the cell is required. The emitting satellite is on the cell ceiling centre. The stations are distributed over a plane 1 meter above the room floor. The area of the cell is bounded by a circle with a given radius. The optical interfaces of the transceivers are considered to be always pointed vertically. The optimization is done for the downward link (satellite to transceiver). The main system physical parameters are presented in table 1.

Parameter	Value
Room Length	12 m
Room Width	12 m
Room Height	4 m
Cell Radius	6 m
Resolution	10 cm
Satellite Position	(0, 0, 0)
Source Array	13 LEDs
Total Emitted Power	152 mW
Receiver Plane	(x, y, -3)
Receiver Active Area	1.0 cm ²
Receiver Sensitivity	-46.1 dBm
Receiver <i>FOV</i>	85 degrees

Table 1 - Physical characteristics of a system with active reflection

Through trial-and-error it has been found that an array of 13 commercially available LEDs emitting a total power of 152 mW would be required to illuminate this cell, assuming a receiver sensitivity of -46.1 dBm typical of a full response Manchester receiver [5]. If other LEDs with more convenient radiation patterns were available the number of LEDs required would be decreased.

The propagation losses were calculated both theoretically and through simulation for a non-optimized emitting pattern [1]. The results obtained through theoretical evaluation and using the simulation package were in total agreement. This confirms that the simulation package is operating correctly. The maximum channel propagation losses were 68.845 dB/cm² at position (6, 0, -3). The maximum and minimum irradiances were -32.18 dBm/cm² and -47.03 dBm/cm², respectively. Thus, the cell dynamic range was 14.85 dB.

Simulation with optimization

As referred previously an array of 13 commercially available LEDs with two different HPBW values, emitting a total power of 152 mW, would be required to illuminate the target cell. The resulting power distribution profile over the coverage cell is shown in figure 3.

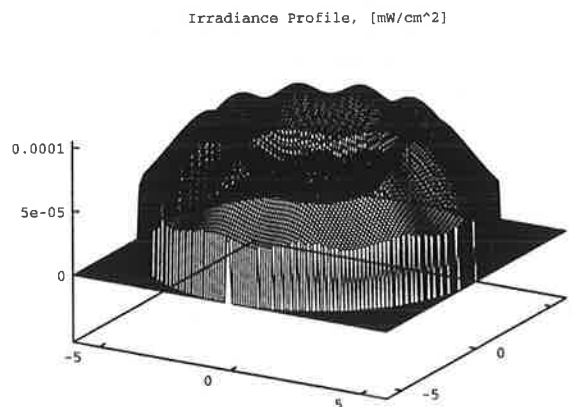


Figure 3 - Power density distribution profile with optimization.

This power distribution was achieved by using two arrays of LEDs with the following characteristics and orientation:

- 11 LEDs ($P_t=12$ mW and $HPBW=14^\circ$) with an elevation angle of 62° and uniformly distributed azimuthal angles, with one of the LEDs with an azimuthal angle of 0° .
- 2 LEDs ($P_t=10$ mW and $HPBW=55^\circ$) pointed down vertically (elevation angle of 0°).

The maximum channel propagation losses are now 65.2 dB/cm² at position $(-6, 0, -3)$. Therefore there was a reduction of approximately 3.7 dB in the maximum channel losses. The dynamic range of the irradiance profile was also reduced to 3.3 dB (maximum and minimum irradiance are now -39.8 dBm/cm² and -43.1 dBm/cm², respectively). These values show the significant improvement that was obtained through the optimization process. Now, we will address the effects of the optimization process on the channel impulse response.

Channel Impulse Response

As referred previously, the knowledge of the channel impulse response is a key factor in the design of high performance wireless communication systems. Here, the channel impulse response is evaluated assuming the room is empty. On the simulation of the channel impulse response, the reflection coefficients of the room walls and ceiling are assumed to be 0.8 and the ceiling reflection coefficient was assumed to 0.3 . These reflection coefficients are typical values for most of the surfaces [2].

Figure 4 shows the impulse response of the channel after optimization when the receiver is at position $(0.0, 0.0, -3.0)$, continuous curve, and also when the receiver is at position $(5.0, 3.4, -3.0)$, dashed curve.

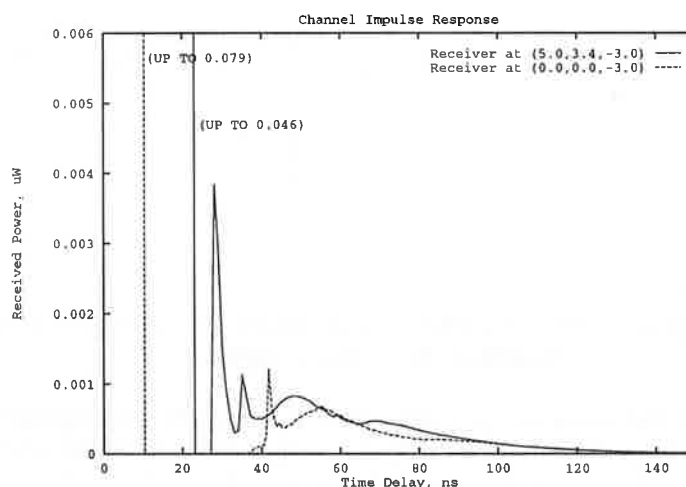


Figure 4 - Channel impulse response.

The results show that pulse spread due to the multipath dispersion may be significant. The associated intersymbol interference will certainly introduce a considerable penalty on systems for baud rates higher than a few Mbit/s. The two curves show also that the channel impulse response changes dramatically with the receiver position.

The contribution of each order of reflection for the total collected power and their effects on the channel bandwidth are summarized on table 2 for the case of the receiver being at position $(5.0, 3.4, -3.0)$. The table presents the results for the optimized and non-optimized cases.

Reflection N°	Optimized System		Non-optimized System	
	Contribution nW - (%)	Bandwidth MHz	Contribution nW - (%)	Bandwidth MHz
0 (LOS)	46.8 - (50.5)	Very Large	30.0 - (39.2)	Very Large
1	13.3 - (14.4)	82.7	6.3 - (11.7)	76.2
2	14.8 - (16.0)	13.1	12.7 - (23.7)	10.6
3	8.1 - (8.7)	8.0	5.9 - (11.6)	7.2
4	5.9 - (6.4)	6.5	4.7 - (8.9)	5.9
5	3.8 - (4.1)	5.7	2.9 - (5.5)	5.2

Table 2 - Influence of the reflection order.

Table 2 shows the small contribution that higher order reflections have on the total collected power. However, for higher orders, the signal arrives with longer delays therefore it reduces drastically the channel bandwidth. This effect is better represented on the frequency domain through the channel transfer function. Figure 5 presents the discrete time Fourier transform of the channel impulse response. The effects of each reflection order on the magnitude response and on the phase response, figure 5a) and 5b), respectively. The DC component increases with the number of reflections considered while the bandwidth decreases. The line of sight impulse response is a delta function and has zero phase. The phase response becomes less linear for simulations considering higher order reflections.

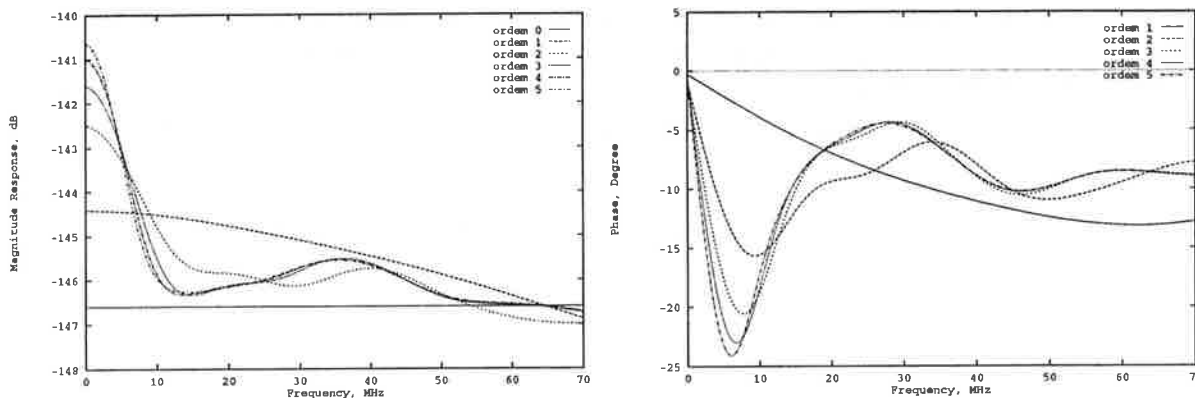


Figure 5 - Effects of higher order reflections on the channel frequency response. a) - Magnitude response. b) - Phase response.

The impulse response of the same room configuration using the non-optimized emitter was also evaluated through simulation. The channel impulse response is different from the one obtained in the optimized case. This fact is specially due to changes on the LOS and first order contributions as the higher order reflections are similar on both cases, see table 2.

The optimization process resulted also on an increase of the channel bandwidth, 5.2 MHz for the non-optimized system and 5.7 MHz for the optimized case. The change on the channel bandwidth depends on the receiver position. Considering the receiver at several different locations the simulations with both, optimized and non-optimized emitter were run. The results show that the optimization process reduces the variation of the LOS and first order contributions with the receiver location. The channel transfer function and bandwidth becomes less dependent on the receiver location. A more detailed study of this issue is required.

B - System with Passive Reflection

This case is representative of indoor infrared systems where the ceiling surface presents good reflection characteristics. Gfeller [2] considered this configuration which he called a diffuse system. The stations are distributed over the room space and have the optical interfaces pointed vertically to the ceiling. The emitting station radiates the infrared signal towards the ceiling which is then reflected to the cell area. The main physical characteristics of the system we will consider for simulation are presented in table 3.

Parameter	Value
Room Length	24 m
Room Width	24 m
Room Height	4 m
Cell Radius	6 m
Resolution	20 cm
Ceiling Reflection Coefficient	0.8
Source Array	15 LEDs
Total Emitted Power	213 mW
Transceivers Plane	(x, y, -3)
Receiver Active Area	1.0 cm ²
Receiver Sensitivity	-46.1 dBm
Receiver <i>FOV</i>	85 degrees

Table 3 - Physical characteristics of a system with passive reflection.

The stations are considered to be distributed over a plane 1 meter above the floor. The cell is assumed circular. On the evaluation of the first order power distribution, the reflections from the room walls are neglected and only the reflections from the ceiling are considered. This represents a worst-case situation since the reflections from the room walls would increase the power collected by the stations.

Three different variants of the system specified above have been considered in reference [1]:

- Non-optimized natural orientation.
- Non-optimized targeted orientation.
- Optimized natural orientation.

The results showed that the optimized system with natural orientation presents several advantages over the other two. Both non-optimized systems present some disadvantages. On the non-optimized system with natural orientation the channel presents high propagation losses and the collected power level presents a very high dynamic range. The non-optimized system with targeted orientation reduces the drawbacks of the previous case. However, it is not practical from the user point of view as the transceiver have to be pointed correctly each time the system is moved.

Thus, we will consider the case of natural orientation where the number, orientation and radiation pattern of the LEDs will be optimized in order to minimize the channel losses. The resulting power distribution profile over the cell area is shown in figure 6. This power distribution was achieved by considering two arrays of LEDs with the following characteristics and orientation:

- 11 LEDs ($P_t=15$ mW and $HPBW=4.5^\circ$) with an elevation angle of 72° and uniformly distributed azimuthal angles, with one of the LEDs with an azimuthal angle of 0° .
- 4 LEDs ($P_t=12$ mW and $HPBW=30^\circ$) with an elevation angle of 53° and uniformly distributed azimuthal angles, with one of the LEDs with an azimuthal angle of 0° .

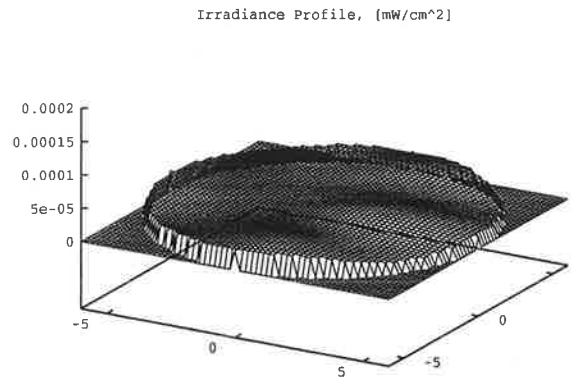


Figure 6 - Irradiance profile for natural orientation and optimization.

The maximum channel losses are now 71.6 dB/cm². A reduction in the maximum propagation losses relative to the non-optimised case of 5.0 dB was achieved.

Channel Impulse Response

The channel impulse response for the optimized system with natural orientation will now be presented in some detail. Figure 7 presents the simulated impulse response and magnitude response of the channel when the receiver is at position (5.0, 3.4, -3.0).

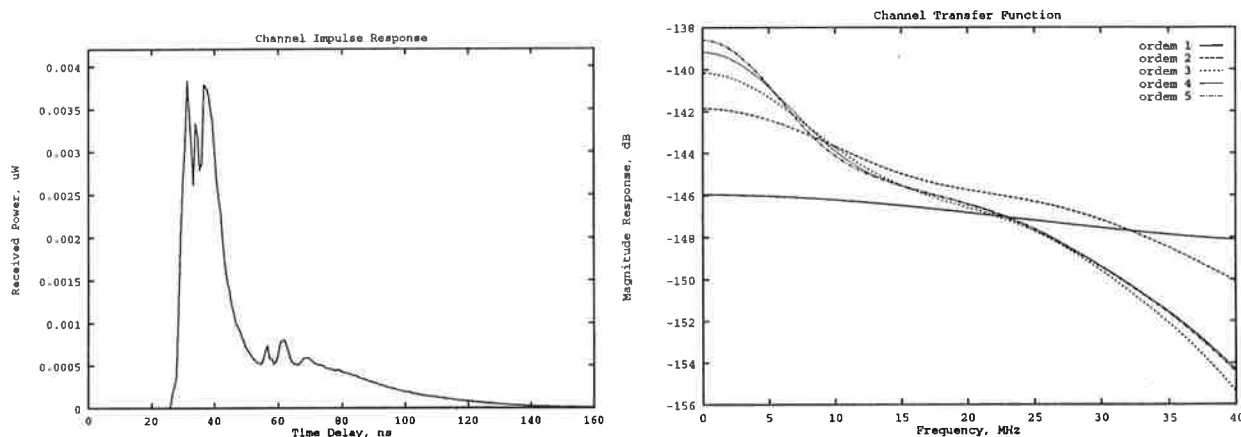


Figure 7: a) - Channel Impulse Response. b) - Channel magnitude response

Figure 7b) presents the magnitude response of the channel considering the influence of each reflection order. There is no curve for the line of sight received power as the system under study assumes passive reflection and energy only goes into the receiver after at least one reflection. The curve labelled **orden 5** corresponds to the channel transfer function and is the discrete Fourier transform of the channel impulse response shown in figure 7a).

The contribution of each order of reflection for the total collected power and their effects on the channel bandwidth are summarised on table 4. The table presents the results for the optimized and non-optimized cases. On the non-optimized case the source is considered to be 1 LED with 60°

emitting a total power of 213 mW, the LED is pointed vertically. All the other system parameters are common to both cases, see table 3.

Table 4 shows that higher order reflections have small contribution on the total collected power. However, for higher orders, the signal arrives with longer delays therefore it reduces drastically the channel bandwidth. The improvements due to the optimization process are not as significant as in the active reflection case due to the signal spreading on the room ceiling.

Reflection N°	Optimized System		Non-optimized System	
	Contribution nW - (%)	Bandwidth MHz	Contribution nW - (%)	Bandwidth MHz
1	50.3 - (25.9)	65.9	42.8 - (48.9)	70.3
2	30.5 - (16.0)	14.3	14.0 - (16.0)	21.0
3	17.3 - (14.7)	8.8	15.7 - (18.0)	8.5
4	11.8 - (10.0)	7.1	8.6 - (9.8)	6.8
5	7.7 - (6.5)	6.0	6.4 - (7.3)	5.7

Table 4 - Influence of the reflection order.

C - Experimental System with Passive Reflection

Now, a practical example of an indoor infrared system using passive reflection is briefly discussed. The system main characteristics used on the simulation are presented in table 3.

Parameter	Value
Room Length	8.8 m
Room Width	7.0 m
Room Height	3.1 m
Resolution	20 cm
Floor Reflection Coefficient	0.6
Back Reflection Coefficient	0.8
Right Reflection Coefficient	0.7
Front Reflection Coefficient	0.8
Left Reflection Coefficient	0.8
Ceiling Reflection Coefficient	0.8
Source Position	(0, 0, -2.1)
Source Array	8 LEDs
Total Emitted Power	120 mW
Transceivers Plane	(x, y, -2.1)
Receiver Active Area	5.0 cm ²
Receiver FOV	85 degrees

Table 3 - Physical characteristics of a system with passive reflection.

With the purpose of assessing the validity of the simulation models, measurements were carried out in a system with the characteristics presented in table 3. This case represents a classroom in our department. The stations are considered to be on a plane 80 centimetre above the floor.

The simulations have started with an evaluation of the channel propagation losses and optimization of the source emitting pattern. For that, the simulations considered only one reflection. After a few

trials, the first order power distribution was roughly constant over the room space. For that, we only used one simple array of LEDs with the following characteristics and orientation:

- 8 LEDs ($P_t = 15$ mW and $HPBW = 4.5^\circ$) with an elevation angle of 55° and uniformly distributed azimuthal angles, with one of the LEDs with an azimuthal angle of 0° .

The power collected at several positions on the room have been simulated considering the power that goes into the receiver up to the 5th order reflection. Two walls of the room are painted with plastic paint, other is a complete window using an aluminium structure and the other has a large green board. The floor presents a high specular reflection component. The simulation results have shown that the contribution of the reflections are very relevant.

The experimental measurements have been done using a prototype developed for a 1 Mbit/s wireless infrared network as part of the ESPRIT.6892 - POWER project. The first measurements showed the power distribution was approximately constant over most of the room space. Therefore, it was decided to measure only the power distribution in one quarter of the room.

With comparison purposes experimental and simulation results are both shown in figure 8. The simulated values are scaled by a factor of 1.2. This fact is not very relevant as we had used typical values for all the surface reflection coefficients.

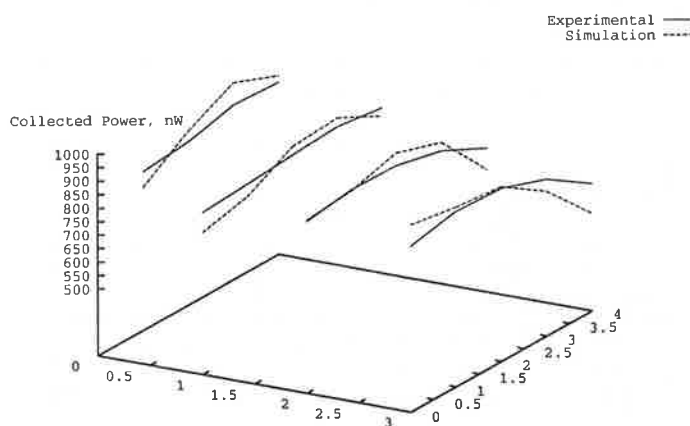


Figure 8 - Comparison of simulated and experimental power collected values.

The figure shows that, apart from the scale factor, experimental and simulated results are in a good concordance. However, there are some discordance between the results, mainly when the receiver approximates the room corners or walls. This difference in the results can be due to the point source model used on the simulation package as near the surfaces the distance between some emitting surfaces and the receiver are very short.

The concordance of the results are very relevant as they confirm the validity of the models used. The optimization process is also working properly as the experimental results of the collected power confirm good uniformity of the power distribution over the room area.

V - Conclusions

The evaluation of the power distribution is very useful on the system power budget. Optimization of the power distribution profile can reduce the maximum channel propagation losses by several dBs and increase slightly the channel bandwidth, at least in some cases.

The multipath dispersion on indoor infrared systems can be significant and have to be considered on the design of systems for baud rates above a few Mbit/s.

On the simulation of indoor optical ~~infrared~~ systems it is very important to consider the reflected signal up to the 4th or 5th order reflections. Those affect mainly the ~~channel~~ bandwidth of the channel as the signal arrives at the receiver with large delay.

The use of passive reflection reduces the effects of shadowing on the system and may also increase the bandwidth.

The experimental measurements were in good concordance with the simulation results which confirm the validity of the models used.

Acknowledgements

The first author would like to thanks to JNICT - Junta Nacional de Investigação Científica e Tecnológica, by its financial support through a Ph.D. grant.

VI - References

- [1] - Lomba, C. R., et al, "*Propagation Losses and Impulse response of the Indoor Optical Channel: A Simulation Package*", Contribution to the IEEE 802.11-93/78, May 1993.
- [2] - Gfeller, F. R., et al, "*Wireless In-House Data Communications Via Diffuse Infrared Radiation*", Proc. IEEE Vol. 67, N°11, November 1979.
- [3] - Pahlavan, K., "*Wireless Intraoffice Networks*", ACM Transactions on Office Information Systems, Vol. 6, N° 3, July 1988.
- [4] - Valadas, R., et al, "*Hybrid (Wireless Infrared/Coaxial) Ethernet Local Area Networks*", Proc. of the IEEE International Conference on Wireless LAN Implementation, Dayton, Ohio, 17-18 September 1992.
- [5] - Barry, R.J., et al. "*Simulation of Multipath Impulse Response for Indoor Wireless Optical Channels*", IEEE Workshop on Wireless Local Area Networks, Worcester, May 1991.
- [6] - Lomba, C., "*Simulation of Multipath Impulse Dispersion on Infrared Communication Systems*", University. of Aveiro, Internal Report, July 1992.
- [7] - Moreira, A. J. C., et al, "*Modulation / Encoding Techniques for Wireless Infrared Transmission*", Submitted to the IEEE 802.11 project May 1993.
- [8] - Siegel, R. and Howell, J. R., "*Thermal Radiation Heat Transfer*", Hemisphere Publishing Corp., Washington, D.C. 1981.

